able explanation for this phenomenon is that the other species (electrons in α-6T and holes in C_{60}) become trapped in extremely low mobility states. The data in Fig. 4 and the energy level lineup in Fig. 2 suggest that the energies of such trap levels are not too far from the appropriate HOMO-LUMO energy levels. Were this not the case, and if the traps were very deep, the complementary behavior seen in these transistors would not be possible. For example, field-induced electrons, instead of occupying high-mobility states in C_{60} (Fig. 3B), might become trapped in lower lying low-mobility trap states in α-6T. The densities of the interface states (at the SiO_2–α-6T and α-6T–C_{60} interfaces) are also low enough not to seriously affect the bending of energy levels (Fig. 3) with bias.

Our observations suggest that heterojunctions based on organic materials have important similarities with their inorganic counterparts, including an approximate conformity with the so-called electron affinity rule, which prescribes the manner in which energy levels line up when a heterojunction is formed (*11*). More important, the transistor behavior indicates that the magnitude of the HOMO-LUMO discontinuities remains substantially unchanged under bias conditions. One of the practical applications of this work is the use of organic transistors in the fabrication of low-power digital circuits. Complementary circuits (which require n-channel and p-channel transistors) dissipate very little power because most of the transistors pass current only for brief periods when they are being switched (*12*); thus, in this application they can offer the dual advantages of lower power dissipation and extended device lifetime. The latter advantage is considered especially beneficial for organic-polymeric transistors.

REFERENCES

1. F. Garnier *et al.*, *Adv. Mater.* **2**, 592 (1990).
2. H. E. Katz, A. Dodabalapur, L. Torsi, A. J. Lovinger, R. Ruel, *Proc. Am. Chem. Soc. Div. Polym. Mater. Sci. Eng.* **72**, 467 (1995).
3. A. Dodabalapur, L. Torsi, H. E. Katz, *Science* **268**, 270 (1995).
4. J. Kastner, J. Paloheimo, H. Kuzmany, in *Springer Series in Solid State Sciences*, H. Kuzmany, M. Mehring, J. Fjink, Eds. (Springer-Verlag, Berlin, 1993), vol. 113, pp. 512–515.
5. R. C. Haddon *et al.*, *Appl. Phys. Lett.* **67**, 121 (1995).
6. C. Hosokawa *et al.*, *ibid.* **62**, 3228 (1993).
7. T. R. Ohno *et al.*, *Phys. Rev. B* **44**, 13747 (1991); G. K. Wertheim and D. N. E. Buchanan, *ibid.* **50**, 11070 (1994); G. K. Wertheim, personal communication.
8. F. Garnier, R. Hajlaoui, A. Yassar, P. Srivastava, *Science* **265**, 1684 (1994).
9. A. Dodabalapur *et al.*, unpublished results.
10. L. Torsi, A. Dodabalapur, H. E. Katz, *J. Appl. Phys.* **78**, 1088 (1995).
11. F. Capasso and G. Margaritondo, Eds., *Heterojunction Band Discontinuities: Device Physics and Applications* (North-Holland, New York, 1987).
12. J. Millman, *Microelectronics: Digital and Analog Circuits and Systems* (McGraw-Hill, New York, 1979).

18 April 1995; accepted 14 July 1995

Observation and Origin of Self-Organized Textures in Agates

Peter J. Heaney* and Andrew M. Davis

One of the most impressive manifestations of spontaneous pattern generation in natural materials is iris agate, which contains submicrometer concentric striations that may cycle several thousand times within an individual specimen. Analysis by secondary ion mass spectroscopy and transmission electron microscopy identified the iris texture as alternating layers of fine-grained, highly defective chalcedony and coarse-grained low-defect quartz. This oscillatory zonation in defect concentration may be ascribed to Ostwald-Liesegang crystallization cycles from silica-rich fluids that are variably polymeric and monomeric. Periodic changes in defect concentration and grain size also are observed with wavelengths of hundreds of micrometers and of centimeters, so that agates reveal textural self-similarity over three length scales.

For centuries natural scientists have marveled at patterns within rocks and minerals that formed without the benefit of external templates, and researchers now are attempting to exploit these textures to infer the conditions that govern crystallization processes. Minerals that exhibit compositional zoning (for example, plagioclase, garnet, and augite) have been studied extensively to determine crystal growth rates and cyclic changes in their depositional environments (*1*). Chemists have investigated periodic and aperiodic oscillatory behavior in systems far from equilibrium to understand nonlinear reaction dynamics (*2*). Agates present one of the most spectacular examples of autonomous pattern generation in nature, and the textures exhibited by these concentrically banded bodies are common to a host of spherulitic materials (*3*). Here, we report an examination of iris banding in agates that reveals oscillations in defect concentration over three length scales; this finding suggests crystallization from fluids with fluctuating degrees of polymerization.

Agates form within gas cavities of volcanic host rocks when microcrystalline chalcedony fibers nucleate on vug walls and grow inward (*4*). Although the popularity of agate as a semiprecious gem derives from its colorful zonation, it is the nonpigmented iris banding that is most remarkable for its rhythmic uniformity. Iris bands appear as striations parallel to the cavity wall and perpendicular to the fiber axes, and thus they generate concentric rings. Cross-polarized light microscopy reveals that iris bands oscillate with respect to refractive index: Bands with indices similar to those of quartz alternate with bands having slightly lower refractive indices, and these oscillations may cycle 8000 times or more within a given sector of an agate (*5*, *6*). The wavelength of the oscillation varies from ~0.1 to 5 μm, and the modulation creates an optical diffraction grating for visible light, giving rise to the iridescence that is the hallmark of museum-quality iris agate (*7*, *8*). Though sometimes obscured by pigmentation, zones with iris banding are present in virtually all agates.

Explanations for the occurrence of oscillatory banding in agate have invoked rhythmic segregation of amorphous opal within chalcedony (*5*) and periodic changes in fiber orientation (*8*). Studies that used powder x-ray diffraction and transmission electron microscopy (TEM) do not support these interpretations (*9*–*11*). Frondel (*12*) has demonstrated by scanning electron microscopy (SEM) that the iris layers with lower refractive indices are more easily etched by hydrofluoric acid. He argued that disparate etching rates result from oscillations in hydroxyl content along the chalcedony fiber length; the more rapidly etched "H" bands are OH-rich and the more resistant "L" bands are OH-poor. Because even trace amounts of hydrogen dramatically weaken quartz crystals, the speciation of hydrogen in quartz has provoked numerous investigations (*13*).

To test the possibility that iris bands represent compositional oscillations along the fiber axes, we examined iris agates by secondary ion mass spectroscopy (SIMS). Iris agates were sectioned parallel to the bands, and elemental variation along the fibers normal to the banding was obtained by tunneling through the iris layers by means of $^{16}O^-$ ion bombardment (Fig. 1) (*14*). The coupled substitution $Al^{3+} + Na^+ \leftrightarrow Si^{4+}$ is well documented in chalcedony (*10*), and it is supported in our results by nearly identical count rates for Al and Na (Fig. 1A). This cation exchange suggests that concentration variations for Al and Na should fall exactly out of phase with those

---

P. J. Heaney, Department of Geological and Geophysical Sciences and Princeton Materials Institute, Princeton University, Princeton, NJ 08544, USA.
A. M. Davis, Enrico Fermi Institute, University of Chicago, 5640 South Ellis Avenue, Chicago, IL 60637, USA.

*To whom correspondence should be addressed.

for Si. However, because the sputtering rates for the H bands were higher than for the L bands, the absolute count rates for all ions varied sympathetically. Nevertheless, some compositional cyclicity with $\lambda \approx 200$ nm becomes evident upon normalization of the ^{27}Al and especially the ^{23}Na concentration profiles to that of ^{28}Si (Fig. 1B), such that slightly elevated impurity concentrations appear in the (more rapidly etched) H bands. No variations in absolute count rates for ^{1}H were discerned in the SIMS profiles. If oscillations in hydroxyl content occur as proposed by Frondel (*12*), the magnitude of the variation must fall below the resolution for hydrogen analysis in these experiments (<0.1 weight % H_2O).

Examination by TEM has revealed more important disparities of a structural nature (*15*). Bright-field images of iris agate (Figs. 2A and 3A) exhibit rhythmic banding with a periodicity of ~200 nm normal to the fiber direction. These bands comprise layers with distinctly different grain sizes and defect concentrations. The coarse-grained zones contain nearly perfect quartz crystals that measure 100 to 1000 nm in diameter; by contrast, the mottled fine-grained lamellae consist predominantly of crystals with diameters of 5 to 10 nm. Differential thinning upon Ar ion bombardment during sample preparation confirmed the bimodal sputtering rates for the L and H bands observed with SIMS, and TEM examination identified the coarsely crystalline layers as the L bands, which are more resistant to chemical and mechanical etching and exhibit refractive indices that coincide with those of quartz.

Light optical microscopy indicates that chalcedony fibers maintain crystallographic continuity as they traverse the iris striations. Consistent with this observation, selected area electron diffraction patterns from neighboring L and H bands (Fig. 2, B and C) exhibit the same zone axes. Consequently, the crystallites in the H bands have the same crystallographic orientation as the larger crystals in adjacent L bands. The diffraction patterns from the H-band crystallites are distinguished from their coarse-grained neighbors in the L bands by the presence of streaks and superperiodic spots. Previous studies have demonstrated that the streaks arise from the random intergrowth of the left- and right-handed enantiomorphs of quartz known as the Brazil twins (*10, 11, 16*). The superperiodic reflections are generated by inclusions of the silica polymorph moganite, which may be idealized as an ordered alternation of left- and right-handed quartz at the unit-cell scale (*17*). Powder x-ray diffraction confirms the presence of moganite, but the intercalation of defect-free quartz layers in iris agate explains the systematically lower moganite contents observed in agatoid silica in comparison with other occurrences of chalcedony (*18*).

Thus, the oscillations that create the L and H banding in iris agate represent modulations between low and high densities of defects, as reflected in impurity distribution, grain size, moganite content, and, most markedly, Brazil twin concentration. This self-organized texture must offer some insight into the mechanism of agate formation, which remains controversial. All models agree that spherulitic chalcedony crystallizes from a fluid that is at least partially polymerized with respect to silica (*19*). By contrast, numerous field and experimental studies have demonstrated that defect-free quartz precipitates from solutions of monomeric silica (*20*). Thus, it seems likely that iris banding reflects variations in the activity of silica in solution at the tips of the growing chalcedony fibers.

One model of agate formation proposes that chalcedony fibers form when short-chain silica polymers are bonded by monomeric bridges (*21*). The assembly occurs through a spiral growth mechanism that is activated by a screw dislocation with burgers vector $\mathbf{b} = n/2[110]$. When n is an odd integer, the dislocation produces a change in handedness (a Brazil twin boundary) in the chalcedony fiber. This growth mechanism can account for several structural disparities between chalcedony and macrocrystalline quartz, such as (i) chalcedony fiber elongation perpendicular rather than parallel to the *c* axis, (ii) periodic twisting of chalcedony fibers, (iii) intergrowth of moganite within chalcedony, and (iv) high densities of Brazil twin boundaries in chalcedony.

If agates crystallize in accordance with this mechanism, then iris bands can be attributed to simple Ostwald-Liesegang crystallization cycles (*22*). Cavity fluids that are partly polymerized rapidly precipitate

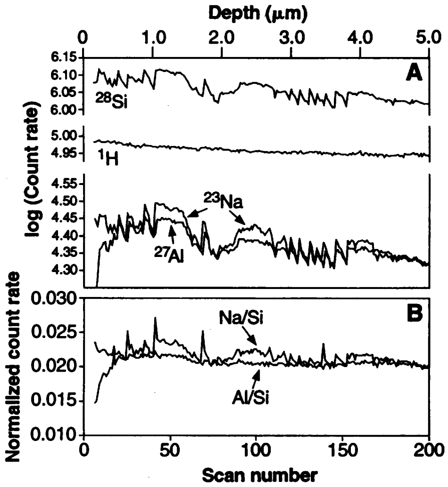

Fig. 1. SIMS data from an agate from Antelope, Oregon (*14*). (**A**) Depth profiles for ^{28}Si, ^{1}H, ^{23}Na, and ^{27}Al normal to the agate bands reveal 200-nm oscillations attributable to differential sputtering of L and H iris layers. No variations in ^{1}H count rates were observed. (**B**) Normalization of Na and Al count rates to Si yields evidence for minor modulations in impurity content along the fiber axes, particularly for Na.

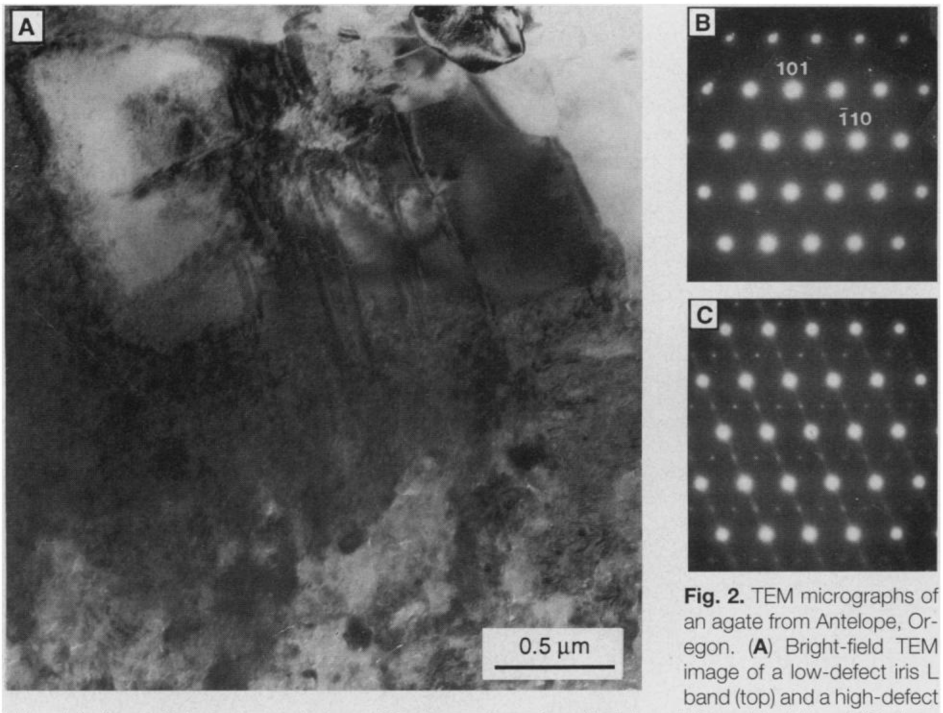

Fig. 2. TEM micrographs of an agate from Antelope, Oregon. (**A**) Bright-field TEM image of a low-defect iris L band (top) and a high-defect H band (bottom). Selected area electron diffraction patterns from the L band (**B**) and the H band (**C**) share the same zone axis, but intense streaking and extra lattice spots in (C) indicate extensive Brazil twins and intergrowths of moganite in the H bands.

spherulitic chalcedony, creating H bands. If depletion of silica near the fiber tips outpaces diffusion toward the tips, then the activity of silica in solution decreases and polymerization is no longer sustained. The resulting monomeric solution precipitates defect-free quartz, generating the iris L bands. Because this crystallization rate is slow (*20*), silica loss near the growing crystal face eventually is overrun by diffusion of silica toward the fiber tips, and the local activity of silica in solution increases. When polymerization is tenable, the spiral growth mechanism is reactivated and rapid crystallization of defective chalcedony ensues.

Although a straightforward supersaturation-nucleation-depletion cycle accounts for oscillatory behavior at the micrometer scale, a complete crystallization model must account for longer-period modulations as well. Figure 3A is a TEM micrograph of a Brazilian agate that exhibits defect-rich and defect-poor iris banding. In a light optical micrograph of the same agate (Fig. 3B), modulations between defect-rich chalcedony and defect-poor quartz with a periodicity of hundreds of micrometers can be observed. These latter oscillations have been described as large iris bands (*6*), but they are structurally distinct because micrometer-sized iris bands are embedded within the larger-scale fine-grained zones. When this agate is viewed in hand specimen (Fig. 3C), a modulation with a centimeter wavelength from exterior fine-grained chalcedony to an interior drusy quartz is observed. Because chalcedony is distinguished from quartz by its extremely high density of Brazil twin boundaries, these textures represent hierarchical oscillations in Brazil twin defect concentrations over wavelengths of micrometers, hundreds of micrometers, and centimeters. Thus, agates exhibit self-similarity over three length scales, each separated by roughly two orders of magnitude. This fractal quality is common to agates from around the world, and it suggests that the crystallization behavior that governs this compositionally simple mineral system is universally complex.

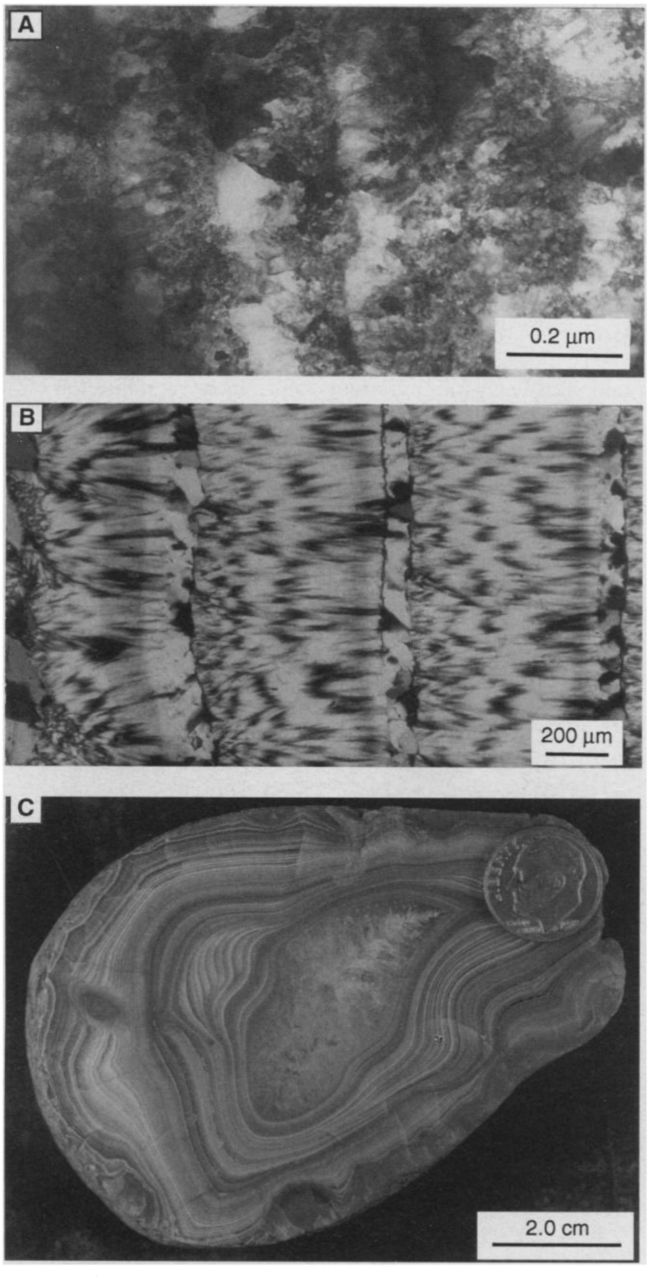

Fig. 3. Cyclic alternation in defect concentration at three length scales in a single agate from Minas Gerais, Brazil (U.S. National Museum 83325). (**A**) Iris banding with periodicity of 0.2 µm observed in TEM bright-field micrograph; (**B**) 700-µm oscillations seen in cross-polarized transmitted light; (**C**) polished cross-section of the agate with transition from chalcedonic exterior to drusy quartz interior over a centimeter scale.

REFERENCES AND NOTES

1. Y. Bottinga, A. Kudo, D. Weill, *Am. Mineral.* **51**, 792 (1966); C. S. Haase, J. Chadam, D. Feinn, P. Ortoleva, *Science* **209**, 272 (1980); C. J. Allègre, A. Provost, C. Jaupart, *Nature* **294**, 223 (1981); R. K. Smith and G. E. Lofgren, *Lithos* **16**, 153 (1983); T. H. Pearce, J. K. Russell, I. Wolfson, *Am. Mineral.* **72**, 1131 (1987); R. J. Reeder, R. O. Fagioli, W. J. Meyers, *Earth Sci. Rev.* **29**, 39 (1990); N. Shimuzu, *ibid.*, p. 27; B. Jamveit, *Am. Mineral.* **76**, 1319 (1991); W. D. Yardley, C. A. Rochelle, A. C. Bamicoat, G. E. Lloyd, *Mineral. Mag.* **55**, 357 (1991).
2. Reviewed in *Chemical Instabilities: Applications in Chemistry, Engineering, Geology, and Materials Science* G. Nicolis and F. Baras, Eds., (Reidel, Dordrecht, Netherlands, 1984), vol. 120; R. J. Field and M. Burger, Eds., *Oscillations and Traveling Waves in Chemical Systems* (Wiley, New York, 1985); L. Györgyi and R. J. Field, *J. Chem. Phys.* **91**, 6131 (1989); S. K. Scott, *Oscillations, Waves, and Chaos in Chemical Kinetics* (Oxford Univ. Press, Oxford, 1994).
3. H. D. Keith and F. J. Padden Jr., *J. Appl. Phys.* **34**, 2409 (1963); F. A. Bovey, in *Macromolecules*, F. A. Bovey and F. H. Winslow, Eds. (Academic Press, New York, 1979), pp. 317–337.
4. C. Frondel, *The System of Mineralogy* (Wiley, New York, 1962), vol. 3; O. W. Flörke, H. Graetsch, B. Martin, K. Röller, R. Wirth, *Neues Jahrb. Mineral. Abh.* **163**, 19 (1991).
5. F. T. Jones, *Am. Mineral.* **37**, 578 (1952).
6. C. Frondel, *ibid.* **63**, 17 (1978).
7. D. Brewster, *Philos. Mag.* **22**, 213 (1843).
8. C. V. Raman and A. Jayaraman, *Proc. Indian Acad. Sci. Sect. A.* **41**, 1 (1955).
9. J. Novák, *Bull. Soc. Fr. Mineral.* **70**, 288 (1947); H. G. Midgley, *Geol. Mag.* **88**, 179 (1951).
10. H. Graetsch, O. W. Flörke, G. Miehe, *Phys. Chem. Miner.* **14**, 249 (1987).
11. P. J. Heaney, D. R. Veblen, J. E. Post, *Am. Mineral.* **79**, 452 (1994). As with many spherulitic crystals, chalcedony fibers in iris agate twist about their growth axes, and the periodicity of this twisting is readily observable in cross-polarized light as an oscillatory extinction pattern known as *Runzelbänderung* or zebraic banding [F. Bernauer, *Neues Jahrb. Mineral. Geol. Palaeontol. Beil.* **55**, 92 (1927)]. However, these extinction bands do not coincide with the iris bands and are separated by tens to hundreds of micrometers.
12. C. Frondel, *Am. Mineral.* **67**, 1248 (1982); *ibid.* **70**, 975 (1985). In some instances three distinct bands with high (H), low (L), and intermediate (M) etching rates were discerned; this combination leads to repetitive three-unit sequences, such as . . . LHMHLHMHL . . ., that are always palindromic.
13. For a review of hydrogen speciation in quartz, see A. K. Kronenberg, *Rev. Mineral.* **29**, 123 (1994).
14. For each depth profile, the $^{16}\mathrm{O}^{-}$ ion beam was rastered over a 90 µm by 90 µm area to ablate a square, flat-bottomed hole parallel to the banding. Ions were collected over only the inner 50% of the rastered area to prevent contamination from the hole edges. Holes measuring 5 µm deep were excavated after 200 scans, and mass numbers 28 (^{28}Si), 27 (^{27}Al), 24 (^{24}Mg), 23 (^{23}Na), and 1 (^{1}H) were sampled after each scan. Sensitivity to hydrogen was estimated from analysis of rhyolite melt inclusions that yield-

ed variations of 1.5 to 6.0 weight % H_2O and rhyolitic host quartz that indicated a blank level of 0.3 weight % H_2O. Four specimens were examined, including two from Minas Gerais, Brazil (U.S. National Museum 117434 and 83325) and two uncataloged samples from Antelope, OR, studied by Frondel (*12*). Elemental oscillations were most pronounced in the Oregon agates, as was consistent with SEM and optical observations of the iris bands. Detection of elemental variations required high precision in the orientation of sections parallel to the banding (within 0.5°).

15. See L. Taijing, X. Zhang, I. Sunagawa, G. W. Groves, *Mineral. Mag.* **59**, 103 (1995). Specimens were sectioned normal to the iris bands at a thickness of 30 μm and further thinned by Ar ion milling. The foils were then sputter-coated with amorphous carbon. TEM was performed with the Philips 400T and Philips CM20 at the General Motors Electron Microbeam Facility, Princeton Materials Institute.
16. G. Miehe, H. Graetsch, O. W. Flörke, *Phys. Chem. Miner.* **10**, 197 (1984); S. L. Cady, H.-R. Wenk, R. Kilaas, D. J. Barber, in *Defects and Processes in the Solid State: Geoscience Applications*, J. N. Boland and J. D. FitzGerald, Eds. (Elsevier, Amsterdam, 1993), pp. 383–400.
17. G. Miehe and H. Graetsch, *Eur. J. Mineral.* **4**, 693 (1992).
18. P. J. Heaney and J. E. Post, *Science* **255**, 441 (1992).
19. For example, see I. Sunagawa and E. Ohta, *Sci. Rep. Tohoku Univ.* **13**, 131 (1976); O. W. Flörke, B. Köhler-Herbertz, K. Langer, I. Tönges, *Contrib. Mineral. Petrol.* **80**, 324 (1982); Y. Wang and E. Merino, *Geochim. Cosmochim. Acta* **54**, 1627 (1990); *Am. J. Sci.* **295**, 49 (1995).
20. H. Harder and W. Flemig, *Geochim. Cosmochim. Acta* **34**, 295 (1970); F. T. Mackenzie and R. Gees, *Science* **173**, 533 (1971); L. A. Williams and D. A. Crerar, *J. Sediment. Petrol.* **55**, 312 (1985); P. M. Dove and J. D. Rimstidt, *Rev. Mineral.* **29**, 259 (1994).
21. P. J. Heaney, *Contrib. Mineral. Petrol.* **115**, 66 (1993).
22. K. H. Stern, *Chem. Rev.* **54**, 79 (1954); P. Ortoleva, E. Merino, C. Moore, J. Chadam, *Am. J. Sci.* **287**, 979 (1987); R. Sultan, P. Ortoleva, F. DePasquale, P. Tartaglia, *Earth Sci. Rev.* **29**, 163 (1990).

23. We thank E. P. Vicenzi, J. E. Post, E. A. Smelik, and D. R. Veblen for helpful discussions. C. Frondel and the U.S. National Museum kindly lent specimens used in this study. Supported by NSF grants EAR92-06031 and EAR94-18031.

21 February 1995; accepted 19 June 1995

Late Glacial Climate Record of Midwestern United States from the Hydrogen Isotope Ratio of Lake Organic Matter

R. V. Krishnamurthy, K. A. Syrup, M. Baskaran, A. Long

A hydrogen isotope time series obtained from an analysis of organic matter extracted from a lake core in Kalamazoo, southwestern Michigan, reveals four distinct isotope stages within the last 12,000 years that can be interpreted in terms of oscillations between cold and warm, dry climates. The most dramatic are a cold phase between 12,000 and 9000 years before present (B.P.), a warm, dry period between 8500 and 2000 years B.P., a cold period between 2000 and 1000 years B.P., and a warming trend since 1000 years B.P. The warming trend of the last 1000 years is comparable in magnitude to the mid-Holocene warm phase.

The stable hydrogen isotope composition [expressed as δD values (*1*)] of plant materials has been used to infer paleoclimatic conditions (*2*). These studies rely on the demonstrable link between the δD of a single plant component, namely the carbon-bound hydrogen of cellulose, and the δD of water used by the plants during their growth. Because the water used by plants is mostly the local meteoric water and the δD of local meteoric water correlates with local mean annual temperature, the δD of cellulose can be translated into climatic factors. In many instances, however, even young sedimentary systems contain negligible amounts of plant remains that can be isolated for this type of study. Extractable sedimentary organic matter, on the other hand, can be found in a wide variety of geologic environments.

Here we report the paleoclimatic information obtained from organic matter (kerogen) extracted from a lake core from southwestern Michigan, analyzed for δD by digestion of the sediments with hydrofluoric and hydrochloric acids (*3*). This procedure is essential to make sure that other hydrogen-containing phases, mostly inorganic minerals, are removed. We assume that (i) the kerogen in lake sediments originates from photosynthesizing aquatic plant biomass that grew in the lake and (ii) that the source of hydrogen for these plants was the local meteoric water recharging the lake. If the δD of kerogen does indeed contain climate information, the scope of its applicability is enormous because kerogen can commonly be extracted from a variety of sediments.

An $\sim$4-m-long core was raised in 1993 from Austin Lake in Kalamazoo (42.10°N, 85.30°W), southwestern Michigan (Fig. 1). This lake is typical of the several "kettle" lakes in the region that were formed by the melting of a mass or masses of ice isolated from the glacier (*4*). At 4.5 km^2, Austin Lake is a relatively large lake for this region and has extensive aquatic vegetation. The sediments are relatively rich in organic carbon (up to 20 weight % on a carbonate-free basis), the source of which must be vegetation in the lake because the lake is isolated from other possible sources of organic matter such as wetlands, streams, and rivers. The lake receives its recharge almost entirely from direct precipitation and is a point of recharge for adjacent ground water.

The H/C ratio (Fig. 2) and the δD values (Fig. 3) of the kerogen samples as a function of age show that lack of significant long-term trends in H/C and δD with age supports the contention that the δD variations are not related to diagenesis (*5*). The δD data can be subdivided into four phases (Table 1 and Fig. 3).

The hydrogen isotope ratio of kerogen in lake sediments with substantial primary productivity reflects the hydrogen of plants that eventually form the source material for sedimentary organic matter. There is ample evidence that the hydrogen in plants is almost entirely derived from the source water, the local precipitation in most cases (*2*). In the present case, we examined if this was true for these lake samples by comparing the δD of kerogen extracted from the top of the core with the δD of environmental water. The δD of kerogen extracted from the surface sample from the top of the core was −80 per mil. For the hydrogen isotope fractionation between the nonexchangeable hydrogen in cellulose extracted from aquatic plants and their environmental water, the δD of the environmental water out of which the lake kerogen was generated should be around −54 per mil (*6*). The one

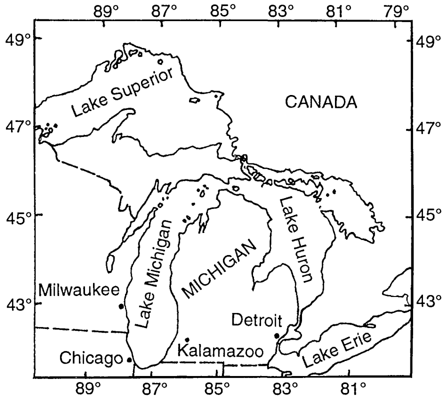

Fig. 1. Map showing Kalamazoo in southwest Michigan, where Austin Lake was cored.

R. V. Krishnamurthy and K. A. Syrup, Department of Geology, Western Michigan University, Kalamazoo, MI 49008, USA.
M. Baskaran, Department of Marine Sciences, Texas A&M University, Galveston, TX 77553–1675, USA.
A. Long, Department of Geosciences, University of Arizona, Tucson, AZ 85721, USA.